HHS Public Access

Author manuscript

Biochemistry. Author manuscript; available in PMC 2018 August 03.

Published in final edited form as:

Biochemistry. 2017 April 04; 56(13): 1836–1840. doi:10.1021/acs.biochem.7b00213.

Probing for and Quantifying Agonist Hydrogen Bonds in $\alpha 6\beta 2$ Nicotinic Acetylcholine Receptors

Michael R. Post[†], **Henry A. Lester**[‡], and **Dennis A. Dougherty**[*,†]

[†] Division of Chemistry and Chemical Engineering, California Institute of Technology, Pasadena, California 91125, United States

[‡] Division of Biology and Biological Engineering, California Institute of Technology, Pasadena, California 91125, United States

Abstract

Designing subtype-selective agonists for neuronal nicotinic acetylcholine receptors is a challenging and significant goal aided by intricate knowledge of each subtype's binding patterns. We previously reported that in $\alpha 6\beta 2$ receptors, acetylcholine makes a functional cation-π interaction with Trp149, but nicotine and TC299423 do not, suggesting a distinctive binding site. This work explores hydrogen binding at the backbone carbonyl associated with $\alpha 6\beta 2$ Trp149. Substituting residue $i + 1$, Thr150, with its α-hydroxy analogue (Tah) attenuates the carbonyl's hydrogen bond accepting ability. At $\alpha 6$(T150Tah)$\beta 2$, nicotine shows a 24-fold loss of function, TC299423 shows a modest loss, and acetylcholine shows no effect. Nicotine was further analyzed via a double-mutant cycle analysis utilizing N'- methylnicotinium, which indicated a hydrogen bond in α6β2 with a ΔΔG of 2.6 kcal/mol. Thus, even though nicotine does not make the conserved cation- π interaction with Trp149, it still makes a functional hydrogen bond to its associated backbone carbonyl.

Graphical Abstract

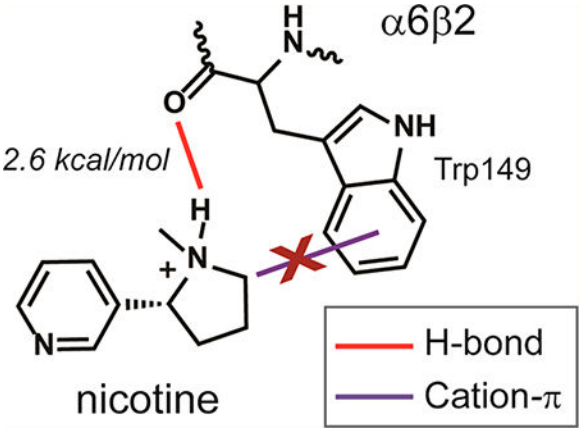

[*]**Corresponding Author** dadougherty@caltech.edu.

Notes

The authors declare no competing financial interest.

The neuronal nicotinic acetylcholine receptors (nAChRs) make up a group of pentameric ligand-gated ion channels (pLGICs) typically found at presynaptic terminals, where they modulate neurotransmitter release.[1–3] There are 11 known subunits *(α2-α7, α9, α10, and β2-β4)* that assemble into pentamers in different combinations.[4] The different subunits share a common topology, and the agonist binding site is found in the extracellular binding region at the interface of two subunits. Different subunit combinations, i.e., different nAChR subtypes, display distinctive functions, pharmacologies, and localizations.[5] While several subtypes are distributed throughout the brain (e.g., $\alpha4\beta2$ and $\alpha7$), others are concentrated in specific regions and expressed by only certain cell types.[6,7] The α6-containing subtypes follow the latter pattern and are prominently expressed in dopaminergic neurons of the ventral tegmental area and the substantia nigra pars compacta, making them promising targets for both Parkinson's disease and addiction.[8–10] In addition, the *α6* subunit is expressed in dorsal root ganglia, where it plays an important role in mechanical allodynia associated with neuropathies and inflammatory injuries.[11] As such, insights into strategies for targeting drugs specifically to *α6*-containing nAChRs would be quite valuable.

Mapping the binding interface is a major step toward that goal. A growing collection of structural data has provided valuable guidance, but it has been less helpful in revealing the subtle features that distinguish particular subtypes. For prototype agonists such as ACh and nicotine (structures shown in Figure 1A), the residues comprising the primary and complementary binding interfaces are conserved among all α and all β subunits, respectively.[12] Therefore, additional precision is required to understand the functional details of neuronal nAChR binding sites.[13] We have established a strategy based on the incorporation of noncanonical amino acids and electrophysiological characterization that allows high-precision characterization of drug-receptor interactions in nAChRs and related systems.[14] Application of this approach to the $\alpha4\beta2$ nAChR, the most common nicotinic receptor in the brain, revealed three key binding interactions: a cation-π interaction with $\alpha4$ Trp149, a hydrogen bond with the backbone carbonyl associated with Trp149, and an additional hydrogen bond between nicotine's pyridine nitrogen and a backbone NH in the $\beta2$ subunit.[15,16] The cation-π interaction at Trp149, which is also termed TrpB as it lies on canonical "loop B" of the primary agonist binding site, has been observed at homologous aromatic residues throughout the nAChR and broader pLGIC families and was later corroborated in recent crystal structures of $\alpha4\beta2$ nAChR, glycine, and serotonin receptors.[17–21] However, recent work using noncanonical amino acid mutagenesis has shown that in the $\alpha6\beta2$ receptor, acetylcholine makes a functionally important cation-π interaction, but nicotine and TC299423 [an agonist that shows some selectivity for $\alpha6\beta2$ receptors[22] (structure shown in Figure 1A)] do not.[23] This binding mode differs from that of the $\alpha4\beta2$ subtype, which suggests the question of what interactions besides a cation-π interaction at Trp149 might be responsible for the binding of nicotine and TC299423 in the $\alpha6\beta2$ nAChR.

This report investigates the role of a possible hydrogen bond between an agonist's amine moiety and the backbone carbonyl associated with TrpB in $\alpha6\beta2$. While quaternary ammonium agonists such as acetylcholine cannot make a hydrogen bond, such interactions have been observed in $\alpha4\beta2$ for nicotine and the smoking cessation drugs varenicline (Chantix) and cytisine (Tabex),[24,25] all of which contain a protonated amine (ammonium ion) that provides the hydrogen bond donor. In each of those instances, evidence of the

hydrogen bond was accompanied by evidence of a cation—π interaction at TrpB; however, because nicotine was not observed to make a strong cation—π interaction at TrpB with $\alpha 6\beta 2$, it was uncertain whether it would make the corresponding hydrogen bond with that tryptophan's backbone carbonyl. Here, structure—function studies using α-hydroxy acid substitution reveal that nicotine indeed makes a functional hydrogen bond with this backbone carbonyl in $\alpha 6\beta 2$. The interaction is further supported and quantified by a double-mutant cycle analysis utilizing N'- methylnicotinium. In contrast, TC299423 shows at best a weak interaction with this carbonyl

RESULTS AND DISCUSSION

α-Hydroxy Acid Substitution at Thr150 in $\alpha 6\beta 2^{\ddagger}$.

All studies make use of the previously described $\alpha 6\beta 2^{\ddagger}$ construct, which contains mutations far removed from the agonist binding site that increase plasma membrane levels, in part, by facilitating transport from the endoplasmic reticulum to the cell surface.[23] To probe for a hydrogen bond to a backbone carbonyl, residue $i + 1$ is mutated to the corresponding α-hydroxy acid (Figure 1B).[26] In both $\alpha 6\beta 2^{\ddagger}$ and $\alpha 4\beta 2$, residue $i + 1$ to Trp149 is Thr150. In the mutation to threonine α-hydroxy acid (Tah), the amide backbone becomes an ester backbone without affecting the side chain (Figure 1C). It is well established that an ester carbonyl is a significantly weaker hydrogen bond acceptor than an amide carbonyl is.[27] In previous studies of several nAChR subtypes, this mutation has produced shifts in EC_{50} ranging from 3- to 27-fold.[13]

The results of substituting $\alpha 6$ Thr150 with Tah are summarized in Table 1. Importantly, ACh, which cannot make a conventional hydrogen bond to the backbone carbonyl, shows no significant effect. This establishes that the function of the receptor has not been degraded in some generic fashion by the backbone mutation. In sharp contrast, nicotine displays a 24-fold increase in EC_{50} (loss of function, dose responses shown in Figure 1D), suggesting it makes a potent hydrogen bond with the backbone carbonyl of TrpB. Perhaps surprisingly, only a 4-fold loss of function was observed for TC299423.

Quantifying the $\alpha 6\beta 2$*—Nicotine Hydrogen Bond.

Our results show that perturbing the backbone carbonyl at TrpB strongly impacts nicotine activation of the $\alpha 6\beta 2^{\ddagger}$ receptor. This is highly suggestive of a hydrogen bond, but other explanations are possible. Also, putting an energetic value on the proposed hydrogen bond is challenging. A classic technique in determining a functional coupling interaction between amino acids in a protein is double-mutant cycle analysis.[28–30] In this type of experiment, the two amino acids of interest are each mutated in a way that would attenuate the proposed interaction, both independently (as single mutants) and simultaneously (as a double mutant). If the change in binding seen in the double mutant is a simple sum of each single mutant—that is, if the energetic effects are additive—the single-mutant perturbations act independently of each other, and the two amino acids do not participate in a functionally coupled interaction. If, on the other hand, the effect of the double mutant proves to be nonadditive, the amino acids are considered to be functionally coupled. The degree to which the double mutant is additive or nonadditive is expressed by an Ω value, which is defined as

the product of the wild-type and double-mutant EC_{50} values divided by the product of the single-mutant EC_{50} values (Figure 2). An Ω value differing from 1 indicates functional coupling between amino acids. As discussed elsewhere, perturbations to EC_{50} resulting from mutations at the agonist binding site can be considered to reflect changes in agonist binding affinities, allowing an Ω valueto be converted to a $\Delta\Delta O$ for the coupling energy between amino acids.[29,31–33]

To assess the nicotine hydrogen bond with the TrpB backbone carbonyl, we designed an analogue of double-mutant cycle analysis (schematic shown in Figure 2). The first mutant in the analysis is the T150Tah substitution that results in an amide-to-ester backbone mutation. The second "mutant" uses a nicotine analogue, wherein the pyrrolidine nitrogen is methylated to yield *N'*-methylnicotinium (N'MeNic in data tables). As a quaternary ammonium, this compound is similar to ACh in that it cannot donate a hydrogen bond. By determining EC_{50} values for each condition (nicotine at the wild type, nicotine at T150Tah, *N'*-methylnicotinium at the wild type, and *N'*-methylnicotinium at T150Tah) and determining whether the double mutant shows an additive loss of function, this mutant cycle will not only further test the hypothesis that nicotine makes a hydrogen bond with the backbone carbonyl of Trp149 but also quantify the strength of the hydrogen bond. We have previously used a similar mutant cycle analysis, one mutation being on the protein the other on the drug, to probe the hydrogen bond involving the pyridine N of nicotine.[30]

As a proof of concept, the double-mutant cycle analysis described above was first performed in the $\alpha4\beta2$ nAChR, because this subtype is more extensively studied and has a better understood binding map for nicotine. At $\alpha4\beta2$, nicotine shows a 27-fold shift in EC_{50} at the T150Tah mutant, a major loss of function (Table 2). When *N'*-methylnicotinium is tested at the wild-type receptor, a 6-fold loss of function is observed. If these two mutations were independent of each other, meaning loss of function was due to an effect other than attenuating the proposed hydrogen bond, an additive loss of function would be expected at the double mutant close to 160-fold. Instead, an EC_{50} of 0.40 μM is observed, which is not meaningfully different from the EC_{50} of *N'*-methylnicotinium at the wild type (0.62 μM) and only a 4-fold loss of function compared to nicotine at the wild type. This lack of additivity is quantified with an Ω value of 42, which when expressed in free energy terms reveals a ΔΔG value of −2.2 kcal/mol. This value is comparable to empirically determined hydrogen bond strengths of N-methylacetamide aggregates in carbon tetrachloride (ΔH° = −4.2 kcal/mol) and benzene ($\Delta H°$ = −3.6 kcal/mol).[34,35]

The same approach was taken in $\alpha6\beta2$*; as noted above, nicotine experiences a 24-fold loss of function at T150Tah. The other single mutant in this analysis, which is *N'*-methylnicotinium at wild-type $\alpha6\beta2^{‡}$, shows an even larger loss of function, with a 38-fold shift in EC_{50}. If these losses in function were not due to hydrogen bonding and instead were independent of each other, the double-mutant fold shift would be additive with a nearly 900-fold increase in EC_{50} with respect to that of the wild type. The double mutant, *N'*-methylnicotinium at T150Tah, has instead an EC_{50} of 1.2, μM, an 11-fold shift away from that of the wild type, showing the effect is nonadditive. Overall, the mutant cycle has an Ω value of 88 and a ΔΔG of −2.6 kcal/mol, suggesting nicotine makes a hydrogen bond in α6β2* that is at least as strong as that seen in $\alpha4\beta2$.

CONCLUSION

These results reveal an interesting diversity among nAChR subtypes. First, consider the binding of nicotine at the two different receptor subtypes, $\alpha4\beta2$ and $\alpha6\beta2$. The binding pattern for $\alpha4\beta2$ is familiar, a strong cation—π interaction with TrpB and a strong hydrogen bond to the associated backbone carbonyl. In $\alpha6\beta2$, the cation—π interaction is absent, so one might conclude that the drug had moved away from TrpB. We now find that nicotine makes a comparably strong hydrogen bond to the backbone carbonyl in $\alpha6\beta2$, a surprising and intriguing binding pattern. Another interesting difference is seen in the consequences of quaternizing nicotine, making it more like the natural agonist ACh. In $\alpha4\beta2$, this has a modest effect on potency (an only 6-fold shift), but in $\alpha6\beta2$, the impact is markedly larger (a 37-fold shift), again suggesting an altered binding orientation.

Finally, our results suggest that TC299423 interacts very weakly with TrpB. There is no evidence of a cation—π interaction, and a backbone mutation has an effect much smaller than that seen for nicotine. These findings should provide valuable guidance to efforts to develop subtype-specific drugs targeting $\alpha6$-containing nAChRs.

MATERIALS AND METHODS

Molecular Biology.

Rat $\alpha6$, $\alpha4$, and $\beta2$ nAChRs were in the pGEMhe vector, a cDNA plasmid optimized for protein expression in *Xenopus* oocytes. Site-directed mutagenesis was performed by polymerase chain reaction using the Stratagene QuikChange protocol and primers ordered from Integrated DNA Technologies (Coralville, IA). Circular cDNA was linearized with SbfI (New England Biolabs, Ipswich, MA) and then transcribed *in vitro* using the T7 mMessage mMachine kit (Life Technologies, Santa Clara, CA), with a purification step after each process (Qiagen, Valencia, CA). Final concentrations were quantified by ultraviolet spectroscopy.

Ion Channel Expression and α-Hydroxy Acid Incorporation.

For optimized expression, $\alpha4$L9′A$\beta2$ and $\alpha6$L9′S$\beta2$L9′$S_{LFM/AAQA}$ were used as the "wild-type" receptor against which further mutations are compared. These are termed $\alpha4\beta2$ and $\alpha6\beta2$*, respectively, throughout for the sake of clarity. For nonsense suppression-based, site-specific noncanonical amino acid incorporation, the cyanomethylester form of threonine α-hydroxy was first synthesized, coupled to the dinucleotide dCA, and enzymatically ligated to UAG suppressor 74-mer THG73 $tRNA_{CUA}$ as previously described.[13] The product was verified by matrix-assisted laser desorption ionization time-of-flight mass spectrometry on a 3-hydrox- ypicolinic acid matrix. *Xenopus laevis* oocytes (stage V—VI) were sourced from both a Caltech facility and Ecocyte Bio Science (Austin, TX). The Tah-tRNA was injected along with T150UAG mRNA into oocytes in a 1:1 volume ratio, with an $\alpha6$:$\beta2$ mRNA mass ratio of 10:1 or an $\alpha4$:$\beta2$ mass ratio of 1:3, resulting in 25 ng each of mRNA and tRNA injected per cell. Cells were incubated for 24—48 h at 18 °C in an ND96 solution [96 mM NaCl, 2 mM KCl, 1 mM $MgCl_2$, and 5 mM HEPES (pH 7.5)] enriched with theophylline, sodium pyruvate, gentamycin, and horse serum. The fidelity of incorporation of Tah was

confirmed by charging tRNA with Thr in a wild-type recovery experiment. Data from these experiments (reported as Thr in Tables 1 and 2) matched wildtype data, reported in previous studies. A read-through/re-aminoacylation test serves as a negative control wherein a 76-mer tRNA is injected alongside mRNA. A lack of current proved there was no detectable re-aminoacylation at the Thr150 site.

N'-Methylnicotinium Synthesis.

Synthesis of N'-methyl- nicotinium was based on previously reported methods.[36] All reagents were purchased from Sigma-Aldrich (St. Louis, MO). In a round-bottom flask, 19.8 mL of (—)-nicotine was added to 250 mL of acetonitrile and excess sodium carbonate. Then, 5.76 mL of methyl iodide was added dropwise while the mixture was being stirred. The reaction mixture was stirred at room temperature for 3 days. The reaction solution was filtered by vacuum, and solids were discarded. Solvent from the filtrate was removed by rotary evaporation until a tan oil remained. Deionized water (50 mL) was added to the oil and dissolved, forming an orange solution. Continuous chloroform extraction was performed on the orange solution for 5 days. The aqueous layer was isolated, and solvent was removed by rotary evaporation upon which crystals formed. The product was recrystallized three consecutive times with hot isopropanol for a yield of >40%. Further purification was achieved by iterative preparative high-performance liquid chromatography (Waters, Milford, MA) using a 100% water solvent profile: ^{1}H NMR (500 MHz, acetonitrile-d_3) δ 8.80 (dd, J = 2.5, 0.8 Hz, 1H), 8.71 (dd, J = 4.8, 1.6 Hz, 1H), 8.12—8.00 (m, 1H), 7.50 (ddd, J = 8.0, 4.8, 0.9 Hz, 1H), 5.06 (dd, J = 11.5, 8.0 Hz, 1H), 3.95— 3.69 (m, 2H), 3.12 (s, 3H), 2.75 (s, 3H), 2.74—2.63 (m, 1H), 2.57—2.42 (m, 1H), 2.39—2.19 (m, 2H).

Whole-Cell Electrophysiological Characterization.

Acetylcholine chloride and (—)-nicotine tartrate were purchased from Sigma-Aldrich, while TC299423 (Targacept) was a generous gift. *N'*-Methylnicotinium iodide was prepared according to the procedure described above. Agonist-induced currents were recorded in two-electrode voltage-clamp mode using the OpusXpress 6000A instrument (Molecular Devices, Sunnyvale, CA) at a holding potential of —60 mV in a running buffer of Ca^2+-free ND96. Agonists were prepared in Ca^2+-free ND96 and delivered to cells via a 1 mL application over 15 s followed by a 2 min wash. EC_{50} values describe the concentration required to activate half the receptors expressed on the cell surface and were determined through dose—response experiments, while fold shifts in EC_{50} are equal to the mutant EC_{50} divided by the wild-type EC_{50}. To derive an EC_{50} value, data from dose—response experiments were normalized to the maximal current response, averaged, and fit to the Hill equation using Kaleidagraph (Synergy Software, Reading, PA), though data are visualized here with Prism (GraphPad Software, La Jolla, CA). Error bars, as well as reported errors for EC_{50} and the Hill coefficient (n_H), are presented as standard errors of the mean.

ACKNOWLEDGMENTS

This work was supported by the National Institutes of Health (NS 34407 and DA019375). M.R.P. was supported by National Institutes of Health/National Research Service Award Training Grant 5 T32 GM07616. We thank Merouane Bencherif and Daniel Yohannes (Targacept) for gifts ofTC299423.

REFERENCES

(1). Quik M , and Wonnacott S (2011) α6β2* and α4β2* Nicotinic Acetylcholine Receptors As Drug Targets for Parkinson's Disease. Pharmacol. Rev 63 938–966.21969327

(2). Wonnacott S (1997) Presynaptic nicotinic ACh receptors. Trends Neurosci 20, 92–98.9023878

(3). Smart TG , and Paoletti P (2012) Synaptic NeurotransmitterGated Receptors. Cold Spring Harbor Perspect. Biol 4, a009662.

(4). Le Nover e N , Corringer P-J , and Changeux J-P (2002) The diversity of subunit composition in nAChRs: Evolutionary origins, physiologic and pharmacologic consequences. J. Neurobiol 53, 447456.

(5). Millar NS (2003) Assembly and subunit diversity of nicotinic acetylcholine receptors. Biochem. Soc. Trans 31, 869–874.12887324

(6). Gotti C , Zoli M , and Clementi F (2006) Brain nicotinic acetylcholine receptors: native subtypes and their relevance. Trends Pharmacol. Sci 27, 482–491.16876883

(7). Zoli M , Pistillo F , and Gotti C (2015) Diversity of native nicotinic receptor subtypes in mammalian brain. Neuropharmacology 96, 302–311.25460185

(8). Quik M , and McIntosh JM (2006) Striatal α6* Nicotinic Acetylcholine Receptors: Potential Targets for Parkinson's Disease Therapy. J. Pharmacol. Exp. Ther 316, 481–489.16210393

(9). Yang K , Jin G , and Wu J (2009) Mysterious a6-containing nAChRs: function, pharmacology, and pathophysiology. Acta Pharmacol. Sin 30, 740–751.19498417

(10). Holladay MW , Dart MJ , and Lynch JK (1997) Neuronal Nicotinic Acetylcholine Receptors as Targets for Drug Discovery. J. Med. Chem 40, 4169–4194.9435889

(11). Wieskopf JS , et al. (2015) The nicotinic α6 subunit gene determines variability in chronic pain sensitivity via cross-inhibition of P2 X 2/3 receptors. Sci. Transí. Med 7, 287ra72–287ra72.

(12). Lester HA , Dibas MI , Dahan DS , Leite JF , and Dougherty DA (2004) Cys-loop receptors: new twists and turns. Trends Neurosci. 27, 329–336.15165737

(13). Van Arnam EB , and Dougherty DA (2014) Functional Probes of Drug-Receptor Interactions Implicated by Structural Studies: Cys-Loop Receptors Provide a Fertile Testing Ground. J. Med. Chem 57, 6289–6300.24568098

(14). Dougherty DA (2000) Unnatural amino acids as probes of protein structure and function. Curr. Opin. Chem. Biol 4, 645–652.11102869

(15). Xiu X , Puskar NL , Shanata JAP , Lester HA , and Dougherty DA (2009) Nicotine binding to brain receptors requires a strong cation-π interaction. Nature 458, 534–53719252481

(16). Tavares XDS , et al. (2012) Variations in Binding Among Several Agonists at Two Stoichiometries of the Neuronal, α4β2 Nicotinic Receptor. J. Am. Chem. Soc 134, 11474–11480.22716019

(17). Dougherty DA (2013) The Cation-π Interaction. Acc. Chem. Res 46, 885–893.23214924

(18). Hassaine G , et al. (2014) X-ray structure of the mouse serotonin 5-HT3 receptor. Nature 512, 276–281.25119048

(19). Miller PS , and Aricescu AR (2014) Crystal structure of a human GABAA receptor. Nature 512, 270–275.24909990

(20). Huang X , Chen H , Michelsen K , Schneider S , and Shaffer PL (2015) Crystal structure of human glycine receptor-α3 bound to antagonist strychnine. Nature 526, 277–280.26416729

(21). Morales-Perez CL , Noviello CM , and Hibbs RE (2016) X-ray structure of the human α4β2 nicotinic receptor. Nature 538, 411–415.27698419

(22). Wall TR (2015) Effects of TI-299423 on Neuronal Nicotinic Acetylcholine Receptors Ph.D. Thesis, California Institute of Technology, Pasadena, CA.

(23). Post MR , Limapichat W , Lester HA , and Dougherty DA (2015) Heterologous expression and nonsense suppression provide insights into agonist behavior at α6β2 nicotinic acetylcholine receptors. Neuropharmacology 97, 376–382.25908401

(24). Puskar NL , Xiu X , Lester HA , and Dougherty DA Two Neuronal Nicotinic Acetylcholine Receptors, α4β4 and α7, Show Differential Agonist Binding Modes. J. Biol. Chem 286, 14618–14627.

(25). Cashin AL , Petersson EJ , Lester HA , and Dougherty DA (2005) Using Physical Chemistry To Differentiate Nicotinic from Cholinergic Agonists at the Nicotinic Acetylcholine Receptor. J. Am. Chem. Soc 127, 350–356.15631485

(26). England PM , Zhang Y , Dougherty DA , and Lester HA (1999) Backbone Mutations in Transmembrane Domains of a LigandGated Ion Channel: Implications for the Mechanism of Gating. Cell 96, 89–98.9989500

(27). Deechongkit S , et al. (2004) Context-dependent contributions of backbone hydrogen bonding to β-sheet folding energetics. Nature 430, 101–105.15229605

(28). Horovitz A (1996) Double-mutant cycles: a powerful tool for analyzing protein structure and function. Folding Des. 1, R121–R126.

(29). Daeffler KN-M , Lester HA , and Dougherty DA (2012) Functionally Important Aromatic-Aromatic and Sulfur-π Interactions in the D2 Dopamine Receptor. J. Am. Chem. Soc 134, 14890–14896.22897614

(30). Blum AP , Lester HA , and Dougherty DA (2010) Nicotinic pharmacophore: The pyridine N of nicotine and carbonyl of acetylcholine hydrogen bond across a subunit interface to a backbone NH. Proc. Natl. Acad. Sci U. S. A 107, 13206–13211.20616056

(31). Colquhoun D (1998) Binding, gating, affinity and efficacy: the interpretation of structure-activity relationships for agonists and of the effects of mutating receptors. Br. J. Pharmacol 125, 923–947.

(32). Marotta CB , Lester HA , and Dougherty DA (2015) An Unaltered Orthosteric Site and a Network of Long-Range Allosteric Interactions for PNU-120596 in α7 Nicotinic Acetylcholine Receptors. Chem. Biol 22, 1063–1073.26211363

(33). Miles TF , Bower KS , Lester HA , and Dougherty DA (2012)A Coupled Array of Noncovalent Interactions Impacts the Function of the 5-HT3A Serotonin Receptor in an Agonist-Specific Way. ACS Chem. Neurosci 3, 753–760.23077719

(34). Klotz IM , and Franzen JS (1962) Hydrogen Bonds between Model Peptide Groups in Solution. J. Am. Chem. Soc 84, 3461–3466.

(35). Davies M , Evans JC , and Jones RL (1955) Molecular interaction and infra-red absorption spectra. Part 4 — Methyl acetamide. Trans. Faraday Soc 51, 761.

(36). Seeman JI , and Whidby JF (1976) The iodomethylation of nicotine. An unusual example of competitive nitrogen alkylation. J. Org. Chem 41, 3824–3826.993886

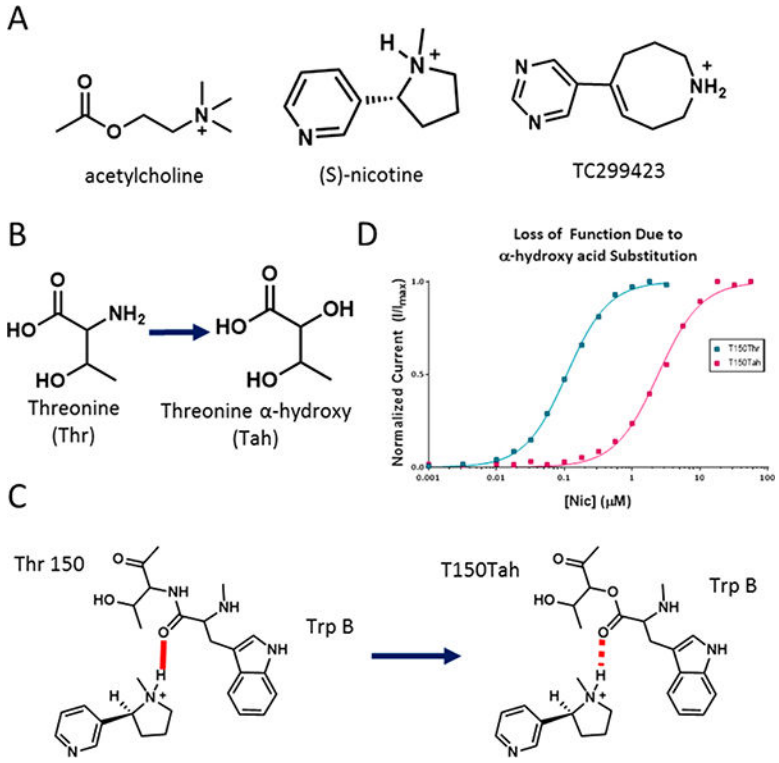

Figure 1.

(A) Agonists used to probe for hydrogen bonds with the Trp149-associated backbone carbonyl in $\alpha 6\beta 2$. (B and C) Probing H- bonds uses the Tah strategy, which effectively mutates the amide backbone into an ester bond. (D) A functional hydrogen bond results in an increase in EC_{50} in the Tah mutant (pink dose-response curve) relative to that of the wild type (blue).

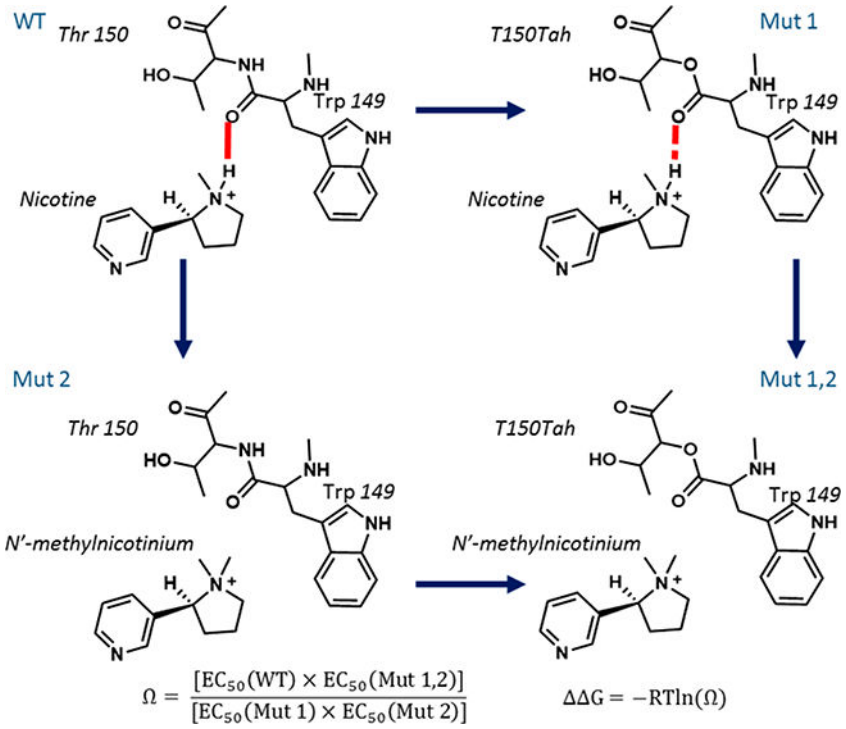

Figure 2.

Schematic of the double-mutant cycle analysis used to confirm and quantify a functional hydrogen bond between nicotine at $\alpha 6\beta 2$ receptors. Equations used to calculate Ω and ΔΔG values are shown.

Table 1.

Hydrogen Bonding at the $\alpha 6\beta 2^*$ TrpB Carbonyl

	EC_{50} (μM)	n_H	I_{max} (μA)	*x*-fold shift	*N*
			Ach		
Thr	0.16 ± 0.01	1.3 ± 0.1	0.32—3.8		10
Tah	0.20 ± 0.01	0.9 ± 0.1	0.48—3.3	1.3	10
			Nicotine		
Thr	0.11 ± 0.01	1.4 ± 0.1	0.19—2.7		16
Tah	2.7 ± 0.1	1.2 ± 0.1	0.09—2.7	24	10
			TC299423		
Thr	0.08 ± 0.01	1.1 ± 0.1	0.21—3.6		11
Tah	0.30 ± 0.01	0.9 ± 0.1	0.12—4.1	3.8	13

Table 2.

Double-Mutant Cycle Analysis of the Nicotine-TrpB Carbonyl Hydroge n Bond

	agonist	T_{150}	EC_{50} (μM)	n_H	I_{max} (μ A)	x-fold shift	N
				$\alpha4\beta2$			
WT	Nic	Thr	0.10 ± 0.01	1.4 ± 0.2	0.05–1.2	1	15
Mut1	Nic	Tah	2.7 ± 0.1	1.3 ± 0.1	0.11–1.2	27	6
Mut2	N'MeNic	Thr	0.62 ± 0.03	1.2 ± 0.1	0.02–0.60	6.2	10
Mut1,2	N'MeNic	Tah	0.40 ± 0.04	1.1 ± 0.1	0.08–0.42	4.0	12
						Ω = 42	
						ΔΔG (kcal/mol) = −2.2	
				$\alpha6\beta2$‡			
WT	Nic	Thr	0.11 ± 0.01	1.4 ± 0.1	0.19–2.7	1	16
Mut1	Nic	Tah	2.7 ± 0.1	1.1 ± 0.1	0.09–2.7	24	10
Mut2	N'MeNic	Thr	4.2 ± 0.2	1.0 ± 0.1	0.10–2.1	38	11
Mut1,2	N'MeNic	Tah	1.1 ± 0.1	0.9 ± 0.1	0.08–1.1	11	10
						Ω = 88	
						ΔΔG (kcal/mol) = −2.6	